Accepted Preprint first posted on 13 May 2014 as Manuscript JOE-14-0054

Sex differences in LXR expression in normal offspring and in rats born to diabetic dams.

SHORT TITLE:

Ontogeny of LXR expression in rat hypothalamus

AUTHOR NAMES AND AFFILIATIONS:

María Sol KRUSE[1] María Cristina VEGA[1] Mariana REY[1] and Héctor COIRINI[1, 2, 3 *]

[1]Laboratorio de Neurobiología, Instituto de Biología y Medicina Experimental (IByME-CONICET), V. de Obligado 2490, (C1428ADN) Ciudad Autónoma de Buenos Aires, Argentina. [2]Departamento de Bioquímica Humana, Facultad de Medicina, Universidad de Buenos Aires, Paraguay 2155, 5to Piso, (C1121ABG) Ciudad Autónoma de Buenos Aires, Argentina. [3]Facultad de Ciencias Medicas, Universidad Católica de Cuyo, Rivadavia, Provincia de San Juan, Argentina.

CORRESPONDING AUTHOR:

Prof. Dr. Héctor Coirini, Laboratorio de Neurobiología, IByME-CONICET, Vuelta de Obligado 2490, C1428ADN Ciudad Autónoma de Buenos Aires, Argentina. Tel.: +54-11-4783-2869 Ext. 250, Fax: +54-11-4786-2564, e-mail: hcoirini@ibyme.conicet.gov.ar

REPRINT REQUESTS SHOULD BE ADDRESSED TO: Dr. Héctor Coirini

KEY WORDS: Glucose tolerance test, AUC, gestational diabetes, insulin resistance

Abstract

Gestational diabetes (GD) alters the normal fetal developing and is related to a diabetogenic effect in the progeny. Liver X receptors (LXR) are considered a potential drug targets for the regulation, treatment or prevention of diabetes. The aim of this study was to evaluate early and late changes of LXR in the hippocampus and hypothalamus of the male and female offspring of control (CO) and diabetic (DO) mothers. We used an experimental model of streptozotocin-induced GD to assess the protein expression of LXRα and LXRβ by Western blot. The tissues were obtained from CO and DO animals at postnatal days 1 (1D), 10 (10D) and 35 (35D) and 9 months (9M). In CO the LXR expression showed significant differences among the groups which were tissue and receptor specific ($p<0.05$). Sex differences in CO were found only in the hypothalamus for LXRβ expression at 35D and 9M ($p<0.05$). When CO vs. DO were compared differences were observed in the majority of the studied groups at 1D (male hippocampus LXRα 31%, LXRβ, 161%, female hippocampus LXRβ, 165%; male hypothalamus, LXRβ 182%, female hypothalamus, LXRα 85% $p<0.05$). However, these differences disappeared later with the exception of LXRβ expression in the male hypothalamus ($p<0.05$). The area under the curve during the glucose tolerance test correlated negatively with LXRβ in CO but not in DO. Moreover, in a male DO subpopulation this correlation was positive as it occurs in intolerant animals. These results suggest that GD affects the hypothalamic LXR expression differently in male and female offspring.

Introduction

Liver X receptor (LXR) α and β are nuclear receptors that trigger various responses to cholesterol overload. These mechanisms include stimulation of reverse cholesterol transport and biliary cholesterol excretion, inhibition of intestinal absorption of dietary cholesterol and suppression of cholesterol synthesis *de novo* (Baranowski 2008). LXR are also involved in glucose homeostasis. The expression of these receptors is increased in pancreatic β cells in type 2 diabetes (Choe, et al. 2007) and LXR stimulation normalize glycemia improving insulin sensitivity in rodent models of type 2 diabetes (Cao, et al. 2003; Commerford, et al. 2007; Laffitte, et al. 2003) without affecting glycemia in nondiabetic animals (Cao et al. 2003; Laffitte et al. 2003).

Both LXR subtypes are present in the central nervous system although the expression of the β subtype is greater than the α subtype (Schmidt, et al. 1999; Whitney, et al. 2002). Nevertheless, the distribution of LXR expression in the brain and their physiological function, in particular with respect to brain control of energy homeostasis, remains to be clarified.

Recently we have demonstrated that LXR expression is altered in the hypothalamus of glucose intolerant rats. Rats fed with a fructose rich diet for 6 weeks develop glucose intolerance, decreased LXRβ levels and increased LXRα expression in the hypothalamus while not affecting the LXR expression in the hippocampus, cerebellum or neocortex (Kruse, et al. 2012a). Moreover, both LXRα and LXRβ expression correlate negatively with serum levels of insulin and triglyceride. The area under the curve (AUC) during glucose tolerance test also correlated negatively with the levels of hypothalamic LXRβ.

Interestingly, the AUC-LXRβ correlation is altered in intolerant rats indicating that the hypothalamus, through this subtype, is especially sensitive to glucose.

Gestational diabetes (GD) is considered a risk factor for developing type 2 diabetes and other metabolic diseases in the offspring (Hillier, et al. 2007; Silverman, et al. 1995). It is known that GD alters the normal fetal development and it produces a diabetogenic effect on the progeny. We have shown that GD affects both the apoptotic and proliferation pathways in the brain from the developing offspring of diabetic rats (Kruse et al. 2012a)

Here we studied the expression of LXRα and LXRβ expression in two brain regions of control rats and rats exposed to hyperglycemia during gestation. These receptor expressions were evaluated at different developmental stages and they were compared between sexes. The results of this study indicate that hypothalamic LXRβ expression, but not LXRα, matures differently in both genders. Moreover, GD induced long-term alterations in LXRβ expression male hypothalamus, but not in females. In these animals the hypothalamic LXRβ/ AUC correlation was also altered compared to controls. Altogether this data may suggest that males exposed to GD may be more susceptible to developing metabolic diseases related to LXR alterations.

Materials and Methods

Experimental animals

Animal procedures have been approved by the Animal Care and Use Ethical Committee of the School of Medicine, University of Buenos Aires, Argentina, in accordance to guidelines defined by the European Communities Council Directive of 24 November 1986 (86/609/EEC) and the National Institutes of Health Guide for the Care and Use of Laboratory Animals procedures. Animals were kept under standard laboratory conditions at 24°C, with light/dark cycles of 12/12 h and food and water *ad libitum*. Sixty days-old female Sprague-Dawley rats weighting 210-260 g (n=8) were placed overnight in cages with males of the same strain. Vaginal smears were examined the next morning and the presence of spermatozoa was considered as day 1 of gestation. Diabetes was induced on gestational day (GD) 3 by a single femoral i.v. injection of 35 mg/Kg streptozotocin (STZ, Sigma-Aldrich) dissolved in saline 0.9% acidified to pH 4.5 using citric acid (n=4) (Coirini, et al. 1980). Vehicle-injected rats served as control (n=4). Forty-eight hours after STZ administration, a pronounced glucosuria (>2 g/100 mL, Diastix; Bayer) and elevation of blood sugar levels of >180 mg/dL were detected in all rats. After delivery, pups were placed with foster mothers. Animals were then sacrificed at different ages by decapitation. The hypothalamus and hippocampus were rapidly dissected, frozen on dry ice and stored at -80 ºC.

Glucose tolerance test

After animals were fasted for 10 h, blood samples were collected from the tail vein and glucose levels were determined by using a commercial strip and a glucometer (OneTouch Ultra, Johnson & Johnson, Argentina). A glucose load was administered by intraperitoneal

injection (2 g/kg body weight) and blood glucose levels were measured at 30, 60, and 120 min post-injection. The area under the glucose curve (AUC) during the glucose tolerance test was calculated using the trapezoidal method of integration.

Western blotting

Homogenates were prepared by sonication in ice-cold lysis buffer (50 mM Tris–HCl, 150 mM NaCl, 2 mM EDTA, 1 mM PMSF, 1 mM Na_3VO_4 and 1% Triton 100, pH 7.4) containing a protease inhibitor cocktail (Roche Diagnostics, Argentina) as previously described (Kruse, et al. 2009a; Kruse, et al. 2009b). 20 μg of protein was separated on 10% SDS-PAGE in Tris-glycine electrophoresis buffer at 120 V for 90 min. Proteins from gels were transferred onto PVDF membranes (Bio-Rad, Argentina) and membranes were blocked with TBS-T (20 mmol/L Tris, pH 7.5; 150 mmol/L NaCl and 0.1% Tween-20) containing 5% of fat-free milk for 1 h. Blocked membranes were incubated with the primary antibody in TBS-T containing 5% fat-free milk at 4ºC overnight. The primary antibodies used were, LXRα (1:1000, Abcam, Cambridge, UK), LXRβ (1:1000, Abcam, Cambridge, UK) and F-Actine (1:1000, Santa Cruz Biotech., USA) (Kruse, et al. 2012b). Immunoblots were then washed with TBS-T three times and incubated at RT for 1 h with the respective HRP-conjugated secondary antibodies (1:5000, GE Healthcare Life Sciences, Argentina). Chemiluminescence was detected with the ECL system (GE Healthcare Life Sciences, Argentina) and exposed to hyperfilm (GE Healthcare Life Sciences, Argentina). All membranes were then stripped and reprobed for F-Actin as a loading control. Signals in the immunoblots were scanned and analyzed by Scion Image software. The amount of target protein was indexed to F-Actin in all cases to ensure correction for the amount of total protein on the membrane.

Statistical analysis

Values are expressed as mean ±S.D. At least three similar but separate experiments were evaluated in all cases containing samples from three to four different animals per treatment. In order to determine the significant differences among variables results were evaluated when corresponded using three way ANOVA and/or two-way ANOVA and then one-way ANOVA followed by Fisher's post-hoc test or Student's t test for two group comparisons. The correlations were also analyzed by ANOVA. In all cases, the Statview Statistical Software (SAS Institute, Inc., Cary, NC, USA; v5.0.1) was used. Differences were considered significant at $P<0.05$.

Results

The expression of LXRα and LXRβ in the hippocampus and hypothalamus was studied in neonatal (1D), infant (10D), juvenile (35D) and adult (9M) rats by Western blot. The results were then compared with the expression of LXR in the offspring of diabetic dams (DO). The gestational diabetes (GD) was induced by a single dose of streptozotocin on gestational day 3 (Kruse et al. 2012a). ANOVA analysis showed that the LXR changes during ontogeny are more drastic for LXRβ (4-8 folds) than LXRα (until 2 folds) in all groups studied (female hippocampus: $F(1,54)=47.70$ $p<0.0001$; male hippocampus: $F(1,79)=16.38$ $p<0.0001$; female hypothalamus: $F(1,54)=9.17$ $p<0.005$; male hypothalamus: $F(1,83)=52.34$ $p<0.0001$) (Fig. 1-4).

LXR expression in the hippocampus.

In the hippocampus of control offspring LXRα expression decreased at 35D of age in females (19% ANOVA, Fisher $p<0.05$) whereas no significant differences were found in males at any age (Fig.1). Regarding LXRβ signal, we observed two peaks at 10D and 9M in male hippocampus (209% and 178%, respectively $p<0.05$) and a significant increase at 9M in female hippocampus (193% $p<0.05$) (Fig.2). Statistical analysis showed no differences between genders (LXRα $F(1,35)=2.65$ $p=0.11$; LXRβ $F(1,42)=0.025$ $p=0.87$).

The LXR expression levels in offspring from control rats (CO) were then compared to rats born from diabetic mothers (DO). We found a significant increase of both LXRα/β expression at 1D (LXRα male hippocampus, 31% $p<0.05$; LXRβ female hippocampus, 165% $p<0.05$; LXRβ male hippocampus, 161% $p<0.005$) indicating that DO at 1D is still affected by the hyperglycemia exposition during gestation (Fig.1 and 2). No further LXR differences between CO and DO were detected at other ages.

LXR expression in the hypothalamus.

In the hypothalamus there was a 63% increase of LXRα expression at 9M of age in males ($p<0.05$) and a 65% increase at 35D in females ($p<0.05$) (Fig.3). LXRβ expression showed a peak at 9M of age in males (796% $p<0.0001$) and two peaks at 10D and 9M in females (298% $p<0.01$ and 342% $p<0.005$, respectively). Sex differences were only found for LXRβ expression in adults (LXRβ 35D and 9M, Student's t-test $p<0.05$; LXRα $F(1,39)=0.002$ $p=0.97$) (Fig.4).

When CO were compared to DO, we found a significant increase at 1D in female LXRα levels (85% $p<0.05$) and in male LXRβ (182% $p<0.005$) (Fig.3 and 4). These differences

disappeared later in life except in the male hypothalamus where LXRβ expression dropped (9M, CO 896% vs. DO 573%, Student's t-test $p<0.05$) (Fig.4). Sex differences were found for LXRβ expression at 35D (Student's t-test $p<0.05$). At 9M the LXRβ difference observed between males and females in control hypothalamus disappeared in DO (Fig.4).

All these results suggest that GD affects males and females differently, having long term consequences only in the male hypothalamus of adult DO.

Glucose tolerance test in adult CO and DO.

The ability to regulate a glucose load was tested in adult five-month-old rats (5M) as DO over that age start to develop glucose intolerance (Boloker, et al. 2002). As with 9M-old animals, 5M-old rats showed decreased LXRβ expression in male DO (26% $p<0.05$) but not in females. After i.p. injection of glucose solution (2 g/kg) two subpopulations were distinguished in the DO group. 38% of male and 36% female DO displayed glucose intolerance showing significant changes at 30, 60 and 120 min (Fig. 5). The AUC during the glucose tolerance test was then calculated using the trapezoidal method of integration (Kruse et al. 2012b). The glucose intolerant animals presented an AUC significantly higher than CO animals and DO animals that did not develop glucose intolerance (animals with AUC >300 vs. animals with AUC <300, respectively) (Fig. 5 insets).

Correlation between LXRβ expression and AUC.

In a previous work we have shown that the AUC correlated negatively with the hypothalamic LXRβ levels but not with LXRα levels. Moreover, in an animal model of

glucose intolerance, LXRβ showed a positive correlation with AUC, indicating an inverse receptor behavior in this experimental condition (Kruse et al. 2012b).

Here, we compared the correlation curves between AUC with the hypothalamic LXRβ levels in 5M CO and DO animals. In accordance to our previous study we observed a negative correlation between AUC and male hypothalamic LXRβ levels in CO (Fig.6A). The slope of the curve obtained was similar as the one we have previously observed in control animals at 3M of age (Kruse et al. 2012b). In female CO, the same correlation was found (Fig.6B). In DO the situation was different. When we combined all the animals together no significant correlation was found in both genders (Fig.6C-D). However, when we separated the animals in two different populations upon their AUC value (glucose tolerant animals AUC <300 or glucose intolerant animals AUC >300) two kinds of regressions were obtained (Fig.7). Male animals that presented AUC below of 300 showed a negative AUC-LXRβ correlation (Fig.7A), while animals with AUC over 300, presented a positive AUC-LXRβ correlation (Fig.7C). In contrast, females with AUC below of 300 showed, as controls, a negative AUC-LXRβ correlation (Fig.7B) while animals with AUC over 300 did not present any correlation (Fig.7D).

Discussion

In this work we found that LXRβ, but not LXRα, is altered in the hypothalamus of adult male offspring born to diabetic dams. In contrast, female offspring did not show long-term LXR changes when compared to controls. No changes were observed between CO and DO

in both male and female hippocampus. Moreover, the correlation between AUC and hypothalamic LXRβ levels is positive in a subpopulation of adult male DO (Fig.7C) suggesting that there is a population in this group capable to developed glucose intolerance associated with an altered hypothalamic LXRβ expression. In contrast, female DO did not show any positive LXRβ-AUC correlation (Fig.7D).

It is now widely accepted that intrauterine exposure to maternal diabetes altered metabolism, increases the risks for obesity and diabetes type 2 in the offspring, in addition to genetic predisposition, and regardless of maternal diabetes type (Dabelea 2007). However, the underlying mechanisms by which exposure to diabetes in uterus increases the risk of offspring obesity are not fully understood. It is been proposed that untreated diabetes in pregnant rats leads to "malprogramming" of hypothalamic neuropeptidergic neurons in offspring, leading to increased orexigenic neuropeptide Y and agouti-related peptide, which could contribute to hyperphagia and later development of overweight (Franke, et al. 2005). In this context, we speculate that the LXRβ alterations observed principally in male DO would probably affect responses of hypothalamic neurons related with energy balance and glucose homeostasis. Little is known about the function of LXR in the hypothalamus. It is been shown that LXRβ$^{-/-}$ but not LXRα$^{-/-}$ mice lose AVP production, in magnocellular neurons of the paraventricular nucleus of the hypothalamus. These animals exhibit polyuria and polydipsia, both features of diabetes insipidus (Gabbi, et al. 2012). In a previous work we found LXR expression in different nuclei of the hypothalamus. The paraventricular and ventromedial nuclei express mainly LXRα whereas the arcuate nucleus expresses LXRβ. Both LXR are present in the median preoptic area (Kruse et al. 2012b). Future studies in

234 our laboratory will focus on elucidating whether LXR is capable of affecting hypothalamic
235 responses.

236 In this paper we found that at 1D most of the DO groups presented an increase in LXR
237 expression, suggesting that LXR may still be affected by hyperglycemia at that age. During
238 development LXR plays a pivotal role in the migration of cortical neurons (Fan, et al.
239 2008). If LXR exerts the same effect in other brain areas (hippocampus and hypothalamus)
240 the alterations observed in DO may influence their brain cytoarchitecture. Indeed, the
241 migration of the neurons from the neuroepithelium in the hypothalamus is controlled by the
242 Notch effector Hes1 (Aujla, et al. 2011), among other factors, and this pathway appears to
243 be regulated by LXR (Kim, et al. 2010).

244 In a recent study we show that uncontrolled GD disrupts both neuronal proliferation and
245 neuronal survival in non-malformed rat embryos at gestational day 19. This is not
246 associated with changes in GFAP levels and heavy neurofilament expression (e.g., NF-200)
247 in the brain from offspring of diabetic rats, indicating that the total number of neurons or
248 glia is no affected by GD at this age (Kruse et al. 2012a). However, since cell proliferation
249 combined with apoptosis sculpts the developing central nervous system (i.e. pruning) it is
250 expected to find enduring neurobiological consequences in the adult brain of DO. In this
251 study we found at least one long-term effect triggered by GD. Adult male DO presented
252 lower expression of LXRβ in the hypothalamus compared to CO at the same age.
253 Moreover, GD increases the appearance of glucose intolerant animals in both sexes that in
254 our assay was 38% for males and 36% for females in 5M old animals (Fig.5). Those
255 animals presented increased AUC and an altered AUC-LXRβ correlation. Even though we
256 found the same proportion of intolerant animals, male DO seems to be more affected by the

hyperglycemic state during development. Adult male DO was the only group showing a significant decrease in LXRβ receptor expression and a subpopulation of this group shows a shift of the AUC-LXRβ correlation curve from negative to positive, as previously observed in a different model of glucose intolerance. In this model rats subjected to a fructose rich-diet for 6 weeks developed hypertriglyceridemia, hyperinsulinemia, and become glucose intolerant, suggesting a progression toward type 2 diabetes. These animals present a decreased hypothalamic LXRβ expression while showing no LXR changes in other brain areas (hippocampus, cerebellum and neocortex). In female DO the situation is different. No long-term LXR changes were found, and even though the AUC-LXRβ correlation was altered in DO compared to CO, no positive correlation was found in this group.

It seems possible that significant sex difference in glucose tolerance rates appears as the animals become older. Male rats gain body weight more rapidly than females, and adipose tissue is preferentially distributed in the abdominal or visceral region (male-pattern of body fat distribution). This distribution carries a much greater risk for metabolic disorders than does adipose tissue distributed subcutaneously (female-pattern) (Wajchenberg, 2000). Ovariectomized rats gain visceral fat with no change of subcutaneous fat (Clegg et al., 2006). Peripheral or central administration of estradiol to these rats restores central leptin sensitivity and changes their body fat distribution to mirror that of intact females. These findings indicate that estrogen regulates body fat distribution. The relative visceral fat volume increase with age more in males than in females (Kotani et al., 1994) suggesting that there is a gender difference in the age-related changes in whole-body fat distribution, especially in the abdominal fat tissues. Moreover, male sex is a risk factor for unfavorable

perinatal outcome (Grill et al., 1991) and those hyperglycemic levels of the mother could results in different effect on the offspring (Regnault et al., 2013). Altogether these results suggest that GD induce different changes depending on the gender, rendering the male progeny more susceptible for developing glucose intolerance and metabolic disturbances related to LXR alterations.

Declaration of interest

The authors declare that there is no conflict of interest that could be perceived as prejudicing the impartiality of the research reported.

Funding

This work was supported by a grant of the National Research Council of Argentina (CONICET) PIP-860 and partially supported by the Catholic University of Cuyo 06CM09. MR was supported by a fellowship from CONICET.

Acknowledgements

We thank Carly McCarthy for comments on the manuscript.

References

Aujla PK, Bora A, Monahan P, Sweedler JV & Raetzman LT 2011 The Notch effector gene Hes1 regulates migration of hypothalamic neurons, neuropeptide content and axon targeting to the pituitary. *Dev Biol* **353** 61-71.

Baranowski M 2008 Biological role of liver X receptors. *J Physiol Pharmacol* **59** Suppl 7 31-55

Boloker J, Gertz SJ & Simmons RA 2002 Gestational diabetes leads to the development of diabetes in adulthood in the rat. *Diabetes* **51** 1499-1506.

Cao G, Liang Y, Broderick CL, Oldham BA, Beyer TP, Schmidt RJ, Zhang Y, Stayrook KR, Suen C, Otto KA, et al. 2003 Antidiabetic action of a liver x receptor agonist mediated by inhibition of hepatic gluconeogenesis. *J Biol Chem* **278** 1131-1136.

Coirini H, Weisenberg L, Tornello S & De Nicola AF 1980 Effect of experimental diabetes on estradiol binding by the anterior pituitary and hypothalamus in ovariectomized rats. *Experientia* **36** 683-685.

Commerford SR, Vargas L, Dorfman SE, Mitro N, Rocheford EC, Mak PA, Li X, Kennedy P, Mullarkey TL & Saez E 2007 Dissection of the insulin-sensitizing effect of liver X receptor ligands. *Mol Endocrinol* **21** 3002-3012.

Choe SS, Choi AH, Lee JW, Kim KH, Chung JJ, Park J, Lee KM, Park KG, Lee IK & Kim JB 2007 Chronic activation of liver X receptor induces beta-cell apoptosis through hyperactivation of lipogenesis: liver X receptor-mediated lipotoxicity in pancreatic beta-cells. *Diabetes* **56** 1534-1543.

Dabelea D 2007 The predisposition to obesity and diabetes in offspring of diabetic mothers. *Diabetes Care* **30** Suppl 2 S169-174.

Fan X, Kim HJ, Bouton D, Warner M & Gustafsson JA 2008 Expression of liver X receptor beta is essential for formation of superficial cortical layers and migration of later-born neurons. *Proc Natl Acad Sci U S A* **105** 13445-13450.

Franke K, Harder T, Aerts L, Melchior K, Fahrenkrog S, Rodekamp E, Ziska T, Van Assche FA, Dudenhausen JW & Plagemann A 2005 'Programming' of orexigenic and anorexigenic hypothalamic neurons in offspring of treated and untreated diabetic mother rats. *Brain Res* **1031** 276-283.

Gabbi C, Kong X, Suzuki H, Kim HJ, Gao M, Jia X, Ohnishi H, Ueta Y, Warner M, Guan Y, et al. 2012 Central diabetes insipidus associated with impaired renal aquaporin-1 expression in mice lacking liver X receptor beta. *Proc Natl Acad Sci U S A* **109** 3030-3034.

Hillier TA, Pedula KL, Schmidt MM, Mullen JA, Charles MA & Pettitt DJ 2007 Childhood obesity and metabolic imprinting: the ongoing effects of maternal hyperglycemia. *Diabetes Care* **30** 2287-2292.

Kim WK, Meliton V, Tetradis S, Weinmaster G, Hahn TJ, Carlson M, Nelson SF & Parhami F 2010 Osteogenic oxysterol, 20(S)-hydroxycholesterol, induces notch target gene expression in bone marrow stromal cells. *J Bone Miner Res* **25** 782-795.

Kruse MS, Barutta J, Vega MC & Coirini H 2012a Down regulation of the proliferation and apoptotic pathways in the embryonic brain of diabetic rats. *Cell Mol Neurobiol* **32** 1031-1037.

Kruse MS, Premont J, Krebs MO & Jay TM 2009a Interaction of dopamine D1 with NMDA NR1 receptors in rat prefrontal cortex. *Eur Neuropsychopharmacol* **19** 296-304.

Kruse MS, Rey M, Barutta J & Coirini H 2009b Allopregnanolone effects on astrogliosis induced by hypoxia in organotypic cultures of striatum, hippocampus, and neocortex. *Brain Res* **1303** 1-7.

Kruse MS, Rey M, Vega MC & Coirini H 2012b Alterations of LXRalpha and LXRbeta expression in the hypothalamus of glucose-intolerant rats. *J Endocrinol* **215** 51-58.

Laffitte BA, Chao LC, Li J, Walczak R, Hummasti S, Joseph SB, Castrillo A, Wilpitz DC, Mangelsdorf DJ, Collins JL, et al. 2003 Activation of liver X receptor improves glucose tolerance through coordinate regulation of glucose metabolism in liver and adipose tissue. *Proc Natl Acad Sci U S A* **100** 5419-5424.

Schmidt A, Vogel R, Holloway MK, Rutledge SJ, Friedman O, Yang Z, Rodan GA & Friedman E 1999 Transcription control and neuronal differentiation by agents that activate the LXR nuclear receptor family. *Mol Cell Endocrinol* **155** 51-60.

Silverman BL, Metzger BE, Cho NH & Loeb CA 1995 Impaired glucose tolerance in adolescent offspring of diabetic mothers. Relationship to fetal hyperinsulinism. *Diabetes Care* **18** 611-617.

Whitney KD, Watson MA, Collins JL, Benson WG, Stone TM, Numerick MJ, Tippin TK, Wilson JG, Winegar DA & Kliewer SA 2002 Regulation of cholesterol homeostasis by the liver X receptors in the central nervous system. *Mol Endocrinol* **16** 1378-1385.

Figure legends

Figure 1. Western blot of LXRα in the hippocampus of male (white bars) and female (gray bars) CO (empty bars) and DO (dotted bars). Data were quantified by densitometric analysis and corrected for the F-actin loading control. Representative pictures of LXR expression and F-actin loading control are shown in the upper panel. Data are presented as mean ± S.D. from at least three independent experiments, n=7–13 animals/group. Significant differences among ages (*) or between CO and DO (#) were determined by one-way ANOVA followed by Fisher's post-hoc test. * $p<0.05$ (male 35D DO and 9M DO vs. 1D DO; female 35D CO vs. 1D CO; female 9M DO vs. 1D DO); # $p<0.05$ (male 1D DO vs. 1D CO)..

Figure 2. Western blot of LXRβ in the hippocampus of male (white bars) and female (gray bars) CO (empty bars) and DO (dotted bars). Data were quantified by densitometric analysis and corrected for the F-actin loading control. Representative pictures of LXR

395 expression and F-actin loading control are shown in the upper panel. Data are presented as
396 mean ± S.D. from at least three independent experiments, n=7–13 animals/group.
397 Significant differences among ages (*) or between CO and DO (#) were determined by one
398 way ANOVA followed by Fisher's post-hoc test. * $p<0.05$ (male 10D CO and 9M CO vs.
399 1D CO; male 35D DO vs. 1D DO; female 9M CO vs. 1D CO and 35D DO vs. 1D DO); #
400 $p<0.05$ (male and female, 1D DO vs. 1D CO).

401

402 **Figure 3.** Western blot of LXRα in the hypothalamus of male (white bars) and female
403 (gray bars) CO (empty bars) and DO (dotted bars). Data were quantified by densitometric
404 analysis and corrected for the F-actin loading control. Representative pictures of LXR
405 expression and F-actin loading control are shown in the upper panel. Data are presented as
406 mean ± S.D. from at least three independent experiments, n=7–13 animals/group.
407 Significant sex differences (§) and differences among ages (*) or between CO and DO (#)
408 were determined by one way ANOVA followed by Fisher's post-hoc test. * $p<0.05$ (male
409 9M CO vs. 1D CO; male 9M DO vs. 1D DO; female 35D CO vs. 1D CO); # $p<0.05$
410 (female 1D DO vs. 1D CO); § $p<0.05$ (male 1D DO vs. female 1D DO).

411

412 **Figure 4.** Western blot of LXRβ in the hypothalamus of male (white bars) and female (gray
413 bars) CO (empty bars) and DO (dotted bars). Data were quantified by densitometric
414 analysis and corrected for the F-actin loading control. Representative pictures of LXR
415 expression and F-actin loading control are shown in the upper panel. Data are presented as
416 mean ± S.D. from at least three independent experiments, n=7–13 animals/group. *

Significant sex differences (§) and differences among ages (*) or between CO and DO (#) were determined by one way ANOVA followed by Fisher's post-hoc test. # $p<0.01$ (male 1D DO vs. 1D CO and 9M DO vs. 9M CO). * $p<0.01$ (male 9M CO vs 1D CO; 9M DO vs. 1D DO; female 10D and 9M CO vs. 1D CO; 10D and 9M DO vs. 1D DO). § $p<0.05$ (male 35D CO vs. female 35D CO; male 35D DO vs. female 35D DO; male 9M CO vs. female 9M CO).

Figure 5. Curves of glucose tolerance in CO and DO. The animals were fasted for 10 h and after the first sampling t = 0 they were intraperitoneally injected with a glucose solution (2 g/kg body weight). Blood samples were drawn from the tail vein at 30, 60 and 120 min after the glucose load. A: Males B: Females. Insets: Numerical integration of the glucose tolerance curve (AUC). DO N: DO animals with AUC <300; DO I: DO animals with AUC >300. Males $F(2;17)=4.21$; $p=0.033$; Females $F(2,13)=9.37$; $p=0.030$ (n= 4-7 animals/group), * $p<0.05$.

Figure 6. Correlation between the area under the curve from the glucose tolerance test (AUC) and the hypothalamic levels of LXRβ in males (A and C, circles) and females (B and D, squares). For the regression plots, the AUC was calculated using the trapezoidal method of integration (Scion Image Software, NIH) and LXR expression was determined by Western blot (n=7–13 animals/group). Each point represents the values corresponding to individual animals from at least three independent experiments (CO, open points. DO, filled points). Significant correlation was found between AUC and LXRβ in control groups

but not in diabetic offspring. One way ANOVA data are shown in each panel. Dotted lines indicate the 95% confidence intervals

Figure 7. Correlation between the area under the curve from the glucose tolerance test (AUC) and the hypothalamic levels of LXRβ in male DO (A and C, circles) and female DO (B and D, squares). The AUC was calculated using the trapezoidal method of integration (Scion Image Software, NIH) and LXR expression was determined by Western blot. Each point represents the values corresponding to individual animals from at least three independent experiments (A and B, animals with AUC <300; C and D, animals with AUC >300). One way ANOVA data are shown in each panel. Dotted lines indicate the 95% confidence intervals.

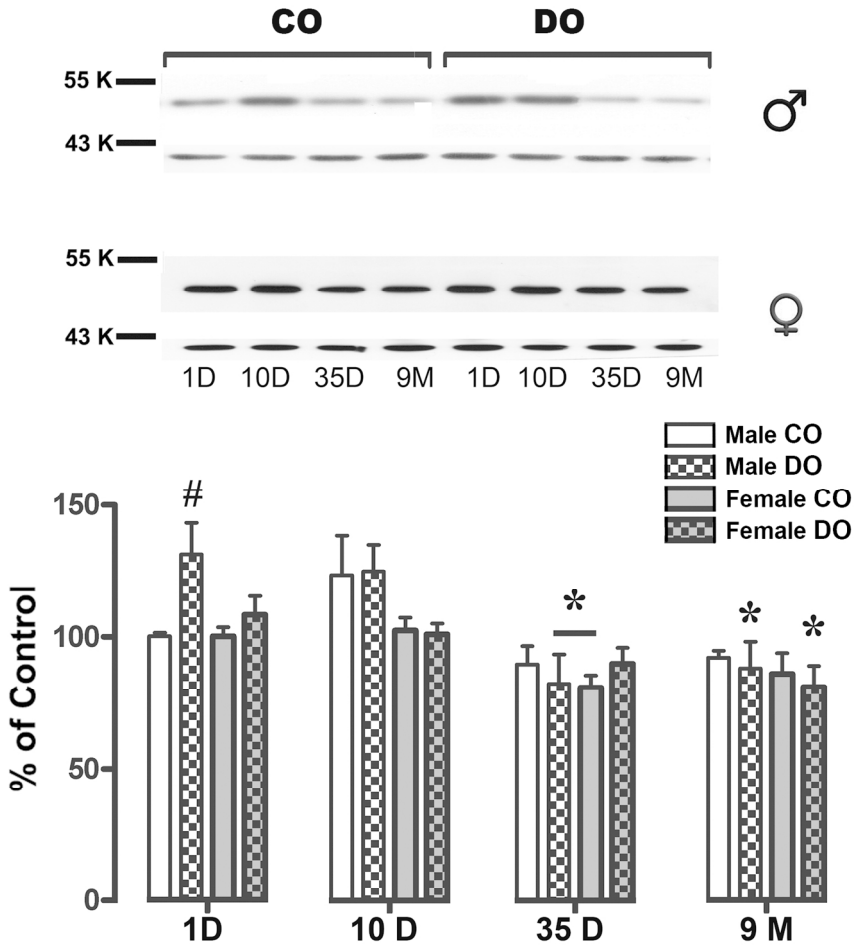

Western blot of LXRα in the hippocampus of male (white bars) and female (gray bars) CO (empty bars) and DO (dotted bars). Data were quantified by densitometric analysis and corrected for the F-actin loading control. Representative pictures of LXR expression and F-actin loading control are shown in the upper panel. Data are presented as mean ± S.D. from at least three independent experiments, n=7–13 animals/group. Significant differences among ages (*) or between CO and DO (#) were determined by one-way ANOVA followed by Fisher's post-hoc test. * $p<0.05$ (male 35D DO and 9M DO vs. 1D DO; female 35D CO vs. 1D CO; female 9M DO vs. 1D DO); # $p<0.05$ (male 1D DO vs. 1D CO).
150x149mm (300 x 300 DPI)

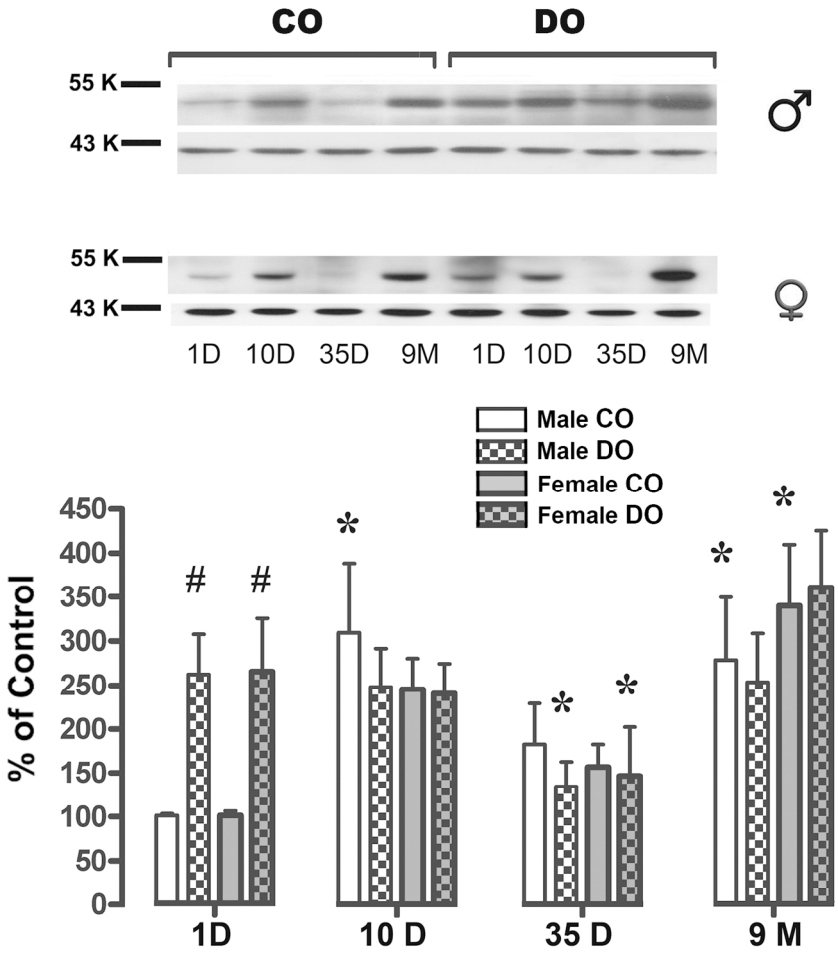

Western blot of LXRβ in the hippocampus of male (white bars) and female (gray bars) CO (empty bars) and DO (dotted bars). Data were quantified by densitometric analysis and corrected for the F-actin loading control. Representative pictures of LXR expression and F-actin loading control are shown in the upper panel. Data are presented as mean ± S.D. from at least three independent experiments, n=7–13 animals/group. Significant differences among ages (*) or between CO and DO (#) were determined by one way ANOVA followed by Fisher's post-hoc test. * $p<0.05$ (male 10D CO and 9M CO vs. 1D CO; male 35D DO vs. 1D DO; female 9M CO vs. 1D CO and 35D DO vs. 1D DO); # $p<0.05$ (male and female, 1D DO vs. 1D CO).
150x149mm (300 x 300 DPI)

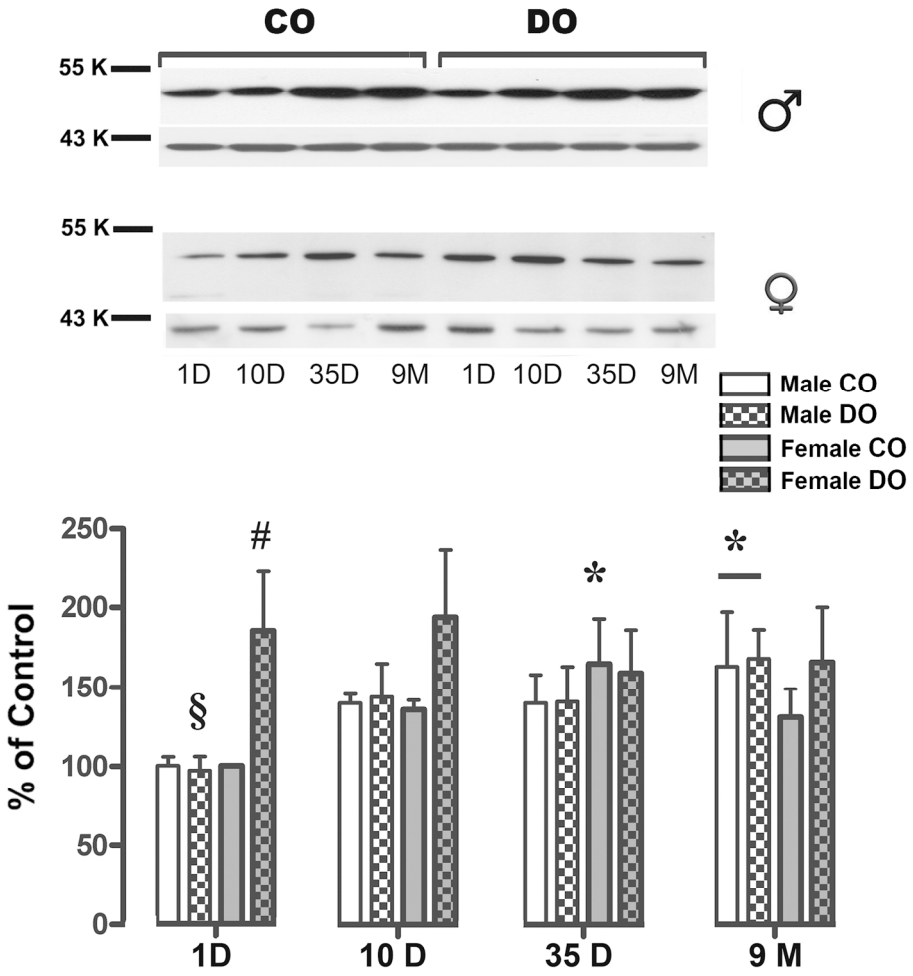

Western blot of LXRα in the hypothalamus of male (white bars) and female (gray bars) CO (empty bars) and DO (dotted bars). Data were quantified by densitometric analysis and corrected for the F-actin loading control. Representative pictures of LXR expression and F-actin loading control are shown in the upper panel. Data are presented as mean ± S.D. from at least three independent experiments, n=7–13 animals/group. Significant sex differences (§) and differences among ages (*) or between CO and DO (#) were determined by one way ANOVA followed by Fisher's post-hoc test. * $p<0.05$ (male 9M CO vs. 1D CO; male 9M DO vs. 1D DO; female 35D CO vs. 1D CO); # $p<0.05$ (female 1D DO vs. 1D CO); § $p<0.05$ (male 1D DO vs. female 1D DO).

150x149mm (300 x 300 DPI)

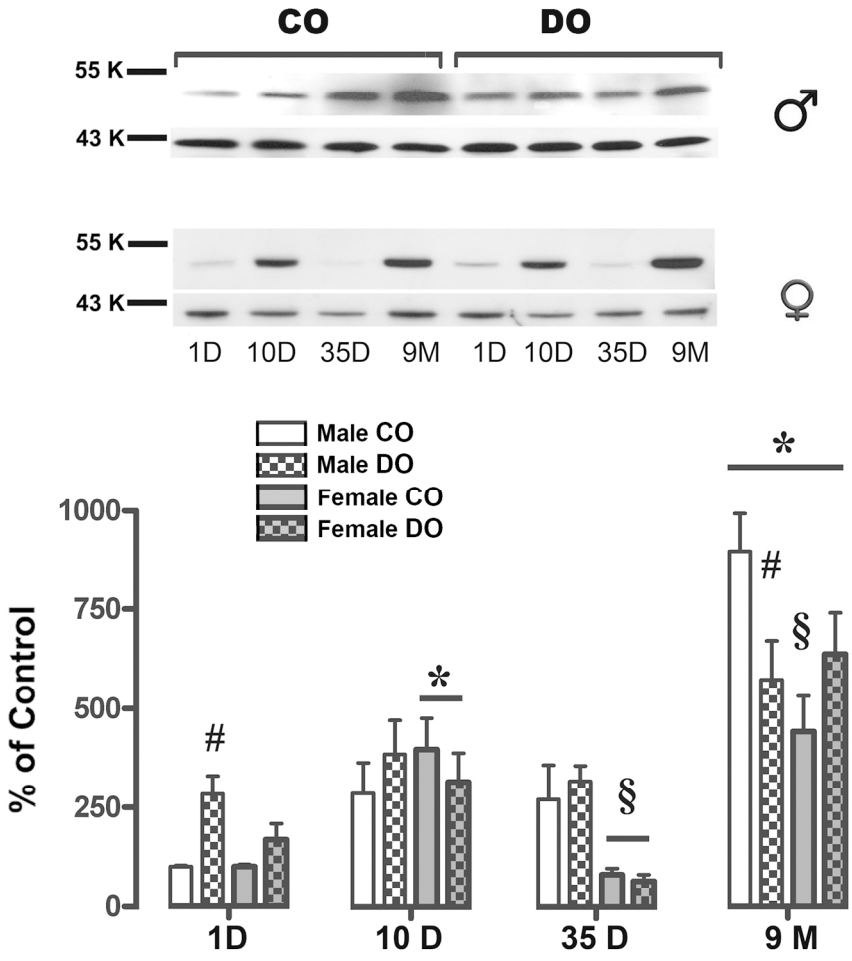

Western blot of LXRβ in the hypothalamus of male (white bars) and female (gray bars) CO (empty bars) and DO (dotted bars). Data were quantified by densitometric analysis and corrected for the F-actin loading control. Representative pictures of LXR expression and F-actin loading control are shown in the upper panel. Data are presented as mean ± S.D. from at least three independent experiments, n=7–13 animals/group. * Significant sex differences (§) and differences among ages (*) or between CO and DO (#) were determined by one way ANOVA followed by Fisher's post-hoc test. # $p<0.01$ (male 1D DO vs. 1D CO and 9M DO vs. 9M CO). * $p<0.01$ (male 9M CO vs 1D CO; 9M DO vs. 1D DO; female 10D and 9M CO vs. 1D CO; 10D and 9M DO vs. 1D DO). § $p<0.05$ (male 35D CO vs. female 35D CO; male 35D DO vs. female 35D DO; male 9M CO vs. female 9M CO).
150x149mm (300 x 300 DPI)

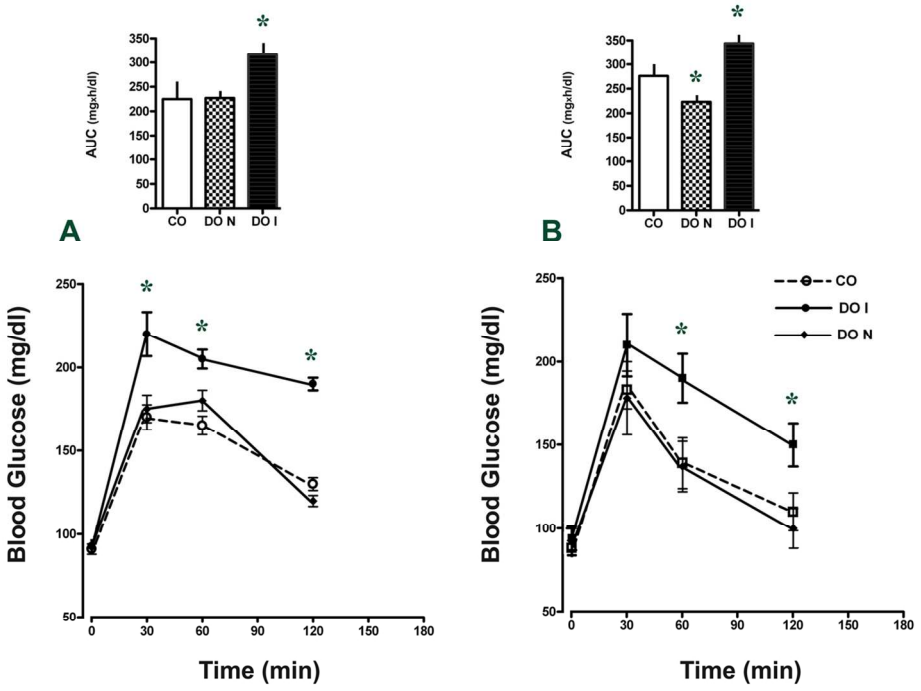

Curves of glucose tolerance in CO and DO. The animals were fasted for 10 h and after the first sampling t = 0 they were intraperitoneally injected with a glucose solution (2 g/kg body weight). Blood samples were drawn from the tail vein at 30, 60 and 120 min after the glucose load. A: Males B: Females. Insets: Numerical integration of the glucose tolerance curve (AUC). DO N: DO animals with AUC<300; DO I: DO animals with AUC>300. Males $F(2;17)=4.21$; $p=0.033$; Females $F(2,13)=9.37$; $p=0.030$ (n = 4-7 animals/group), * $p < 0.05$.
129x98mm (300 x 300 DPI)

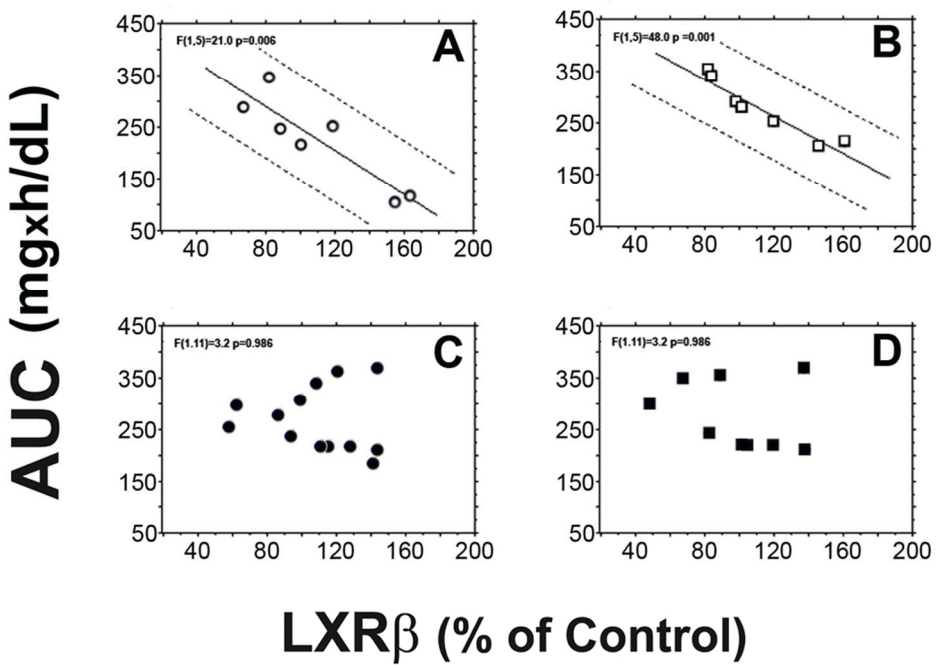

Correlation between the area under the curve from the glucose tolerance test (AUC) and the hypothalamic levels of LXRβ in males (A and C, circles) and females (B and D, squares). For the regression plots, the AUC was calculated using the trapezoidal method of integration (Scion Image Software, NIH) and LXR expression was determined by Western blot (n=7–13 animals/group). Each point represents the values corresponding to individual animals from at least three independent experiments (CO, open points. DO, filled points). Significant correlation was found between AUC and LXRβ in control groups but not in diabetic offspring. ANOVA data are shown in each panel. Dotted lines indicate the 95% confidence intervals
99x73mm (300 x 300 DPI)

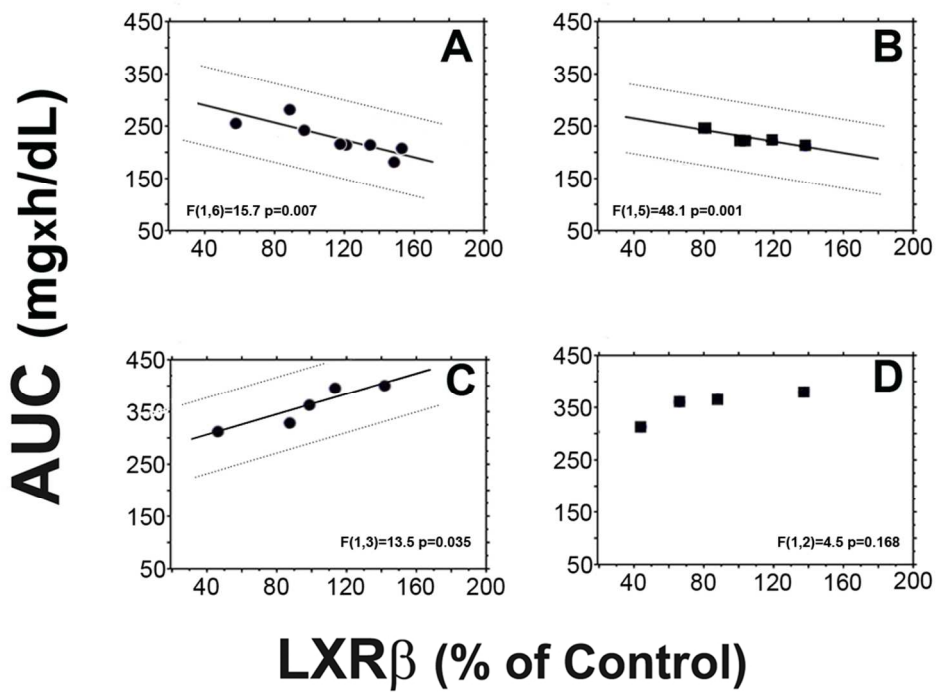

Correlation between the area under the curve from the glucose tolerance test (AUC) and the hypothalamic levels of LXRβ in male DO (A and C, circles) and female DO (B and D, squares). The AUC was calculated using the trapezoidal method of integration (Scion Image Software, NIH) and LXR expression was determined by Western blot. Each point represents the values corresponding to individual animals from at least three independent experiments (A and B, animals with AUC<300; C and D, animals with AUC>300). ANOVA data are shown in each panel. Dotted lines indicate the 95% confidence intervals.
99x72mm (300 x 300 DPI)